Electronic Supplementary Information

Rational design of time-resolved turn-on fluorescence sensors: exploiting delayed fluorescence for hydrogen peroxide sensing

Young Hoon Lee,[a] Saibal Jana,[b] Heechai Lee,[a] Sang Uck Lee,*[b] and Min Hyung Lee*[a]

[a] Department of Chemistry, University of Ulsan, Ulsan 44610, Republic of Korea

[b] Department of Bionano Technology and Department of Chemical and Molecular Engineering, Hanyang University, Ansan 15588, Republic of Korea

Contents

1. Experimental

1.1. General considerations

All operations were performed under an inert nitrogen atmosphere using standard Schlenk and glovebox techniques. Anhydrous-grade solvents (Aldrich) were dried over activated molecular sieves (5Å). Spectrophotometric-grade toluene, THF, and ethanol were used as received from Merck. Commercial reagents were used without further purification after purchase. Deuterated solvents from Cambridge Isotope Laboratories were used. NMR spectra were recorded on a Bruker AM 300 (300.13 MHz for ^{1}H, 75.48 MHz for ^{13}C, 96.29 MHz for ^{11}B, and 121.49 MHz for ^{31}P) spectrometer at ambient temperature. Chemical shifts are given in ppm, and are referenced against external Me_4Si (^{1}H, ^{13}C), $BF_3{\cdot}OEt_2$ (^{11}B), and 85% H_3PO_4 (^{31}P). Elemental analyses were performed on a Flash 2000 elemental analyzer (Thermo Scientific). Melting (mp) points were measured by Melting Point Apparatus SMP30 (Stuart Equipment). Cyclic voltammetry experiments were performed using an Autolab/PGSTAT101 system.

1.2. Synthesis

9-(2,5-Dibromophenyl)-9*H*-carbazole

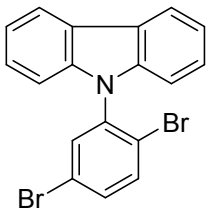

Sodium hydride (60% dispersion in mineral oil, 0.35 g, 8.75 mmol) was washed with *n*-hexane twice, dried, and dispersed in dry DMF (15 mL) under an nitrogen atmosphere. A solution of 9*H*-carbazole (1.3 g, 7.77 mmol) in dry DMF (10 mL) was slowly added to the suspension at room temperature. The mixture was stirred for 2 h and 1,4-dibromo-2-fluorobenzene (2.0 g, 7.88 mmol) in dry DMF (10 mL) was added to this solution. The mixture was heated at 110 °C overnight. After cooling down to room temperature, cold water (250 mL) was slowly added and a turbid white mixture was extracted with diethyl ether (50 mL × 3). The combined ether layer was washed with water (100 mL × 3). The organic layer was dried over $MgSO_4$, filtered, and concentrated under reduce pressure. The crude product was purified by silica gel column chromatography using *n*-hexane as an eluent to give 9-(2,5-dibromophenyl)-9*H*-carbazole as a white powder (Yield: 2.56 g, 81%). ^{1}H NMR ($CDCl_3$): δ 8.14 (d, J = 7.7 Hz, 2H), 7.72 (d, J = 8.6 Hz, 1H), 7.63 (d, J = 2.3 Hz, 1H), 7.54 (dd, J = 8.6, 2.3 Hz, 1H), 7.14 (td, J = 7.5, 1.2 Hz, 2H), 7.30 (td, J = 7.5, 0.6 Hz, 2H), 7.07 (d, J = 8.1 Hz, 2H). ^{13}C NMR ($CDCl_3$): δ 140.4, 138.1, 135.2, 134.0, 133.2, 126.0, 123.33, 122.6, 121.6, 120.4, 120.3, 109.9.

9-(5-Bromo-2-(diphenylphosphino)phenyl)-9*H*-carbazole (1a)

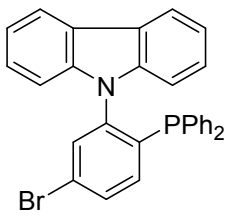

To a solution of 9-(2,5-dibromophenyl)-9*H*-carbazole (0.50 g, 1.25 mmol) in dry ether (30 mL) was added dropwise *n*-BuLi (0.5 mL, 1.25 mmol) at −78 °C. The reaction mixture was stirred at −78 °C for 1 h and then chlorodiphenylphosphine ($ClPPh_2$, 0.23 mL, 1.28 mmol) in dry ether (10 mL) was slowly added. After stirring at room temperature overnight, the resulting yellow solution was quenched by the addition of a saturated aqueous NH_4Cl solution (50 mL), extracted with diethyl ether (30 mL × 3), and washed with water (50 mL × 3). The combined organic layer was dried over $MgSO_4$, filtered, and concentrated under reduced pressure. The crude product was purified by silica gel column chromatography using CH_2Cl_2/*n*-hexane (1:3, v/v) as an eluent to give **1a** as a white powder (Yield: 0.46 g, 75%). ^{1}H NMR (CD_2Cl_2): δ 8.16–8.02 (m, 2H), 7.65 (dd, J = 8.3, 2.0 Hz, 1H), 7.54 (dd, J = 3.8, 2.0 Hz, 1H), 7.32–7.15 (m, 11H), 7.10 (td, J = 7.9, 1.6 Hz, 4H), 6.90–6.87 (m, 2H). ^{13}C NMR (CD_2Cl_2): δ 143.3, 143.0, 142.0, 140.1, 139.9, 136.9, 136.2, 136.1, 134.3, 134.0, 133.6, 133.6, 132.8, 129.4, 129.0, 128.9, 126.2, 124.5, 123.6, 120.5, 120.3, 110.8, 110.7 (Ar–*C*). ^{31}P NMR (CD_2Cl_2): δ −17.5 (s).

9-(5-Bromo-2-(diisopropylphosphino)phenyl)-9*H*-carbazole (2a)

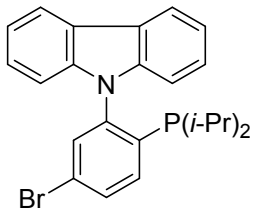

This compound was prepared in a manner analogous to the synthesis of **1a** using 9-(2,5-dibromophenyl)-9*H*-carbazole (0.80 g, 0.93 mmol), *n*-BuLi (0.8 mL, 2.0 mmol), and chlorodiisopropylphosphine ($ClP(i\text{-}Pr)_2$, 0.32 mL, 2.0 mmol) to give **2a** as a white powder (Yield: 0.50 g, 57%). ^{1}H NMR (CD_2Cl_2): δ 8.19 (d, J = 7.7 Hz, 2H), 7.77 (dd, J = 8.3, 2.0 Hz, 1H), 7.70 (dd, J = 8.3, 1.3 Hz, 1H), 7.59 (dd, J = 3.2, 2.0 Hz, 1H), 7.43 (td, J = 7.5, 1.2 Hz, 2H), 7.33 (td, J = 7.4, 0.9 Hz, 2H), 7.12 (d, J = 8.1 Hz, 2H), 2.01 (septet, J = 6.9 Hz, 2H, isopropyl–C*H*), 1.06–0.85 (m, 12H, isopropyl–CH_3). ^{13}C NMR (CD_2Cl_2): δ 145.4, 145.1, 142.4, 137.5, 137.1, 136.1, 136.0, 133.4, 133.3, 132.1, 126.2, 124.5, 123.6, 120.6, 120.3, 111.3, 111.2 (Ar–*C*), 24.7, 24.5, 20.6, 20.3, 19.9, 19.8 (isopropyl–*C*). ^{31}P NMR (CD_2Cl_2): δ −6.4 (s).

9-(5-(Dimesitylboryl)-2-(diphenylphosphino)phenyl)-9*H*-carbazole (C*zm*BP, 1b)

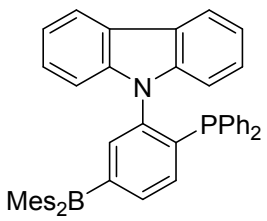

To a solution of **1a** (0.20 g, 0.40 mmol) in dry ether (15 mL) was added dropwise *n*-BuLi (0.15 mL, 0.40 mmol) at −78 °C. The reaction mixture was stirred at −78 °C for 1 h and then Mes_2BF (0.11 g, 1.2 mmol) in dry ether (5 mL) was slowly added. After stirring at room temperature overnight, the resulting yellow solution was concentrated under reduced pressure. The crude product was purified by silica gel column chromatography using CH_2Cl_2/*n*-hexane (1:20, v/v) as an eluent to give C*zm*BP (**1b**)

as a yellow powder (Yield: 0.20 g, 74%). ^{1}H NMR (CD_2Cl_2): δ 8.03 (dd, J = 6.3, 2.1 Hz, 2H), 7.54 (dd, J = 7.7, 1.2 Hz, 1H), 7.41 (dd, J = 4.4, 1.1 Hz, 1H), 7.29 (dd, J = 7.7, 3.4 Hz, 1H), 7.26–7.13 (m, 10H), 7.08 (td, J = 7.9, 1.6 Hz, 4H), 6.86–6.73 (m, 6H, Ar–*H* and Mes–*H*), 2.23 (s, 6H, Mes–CH_3), 2.03 (s, 12H) (Mes–CH_3). ^{13}C NMR (CD_2Cl_2): δ 145.0, 144. 8, 142.2, 142.2, 141.5, 141.2, 139.8, 137.4, 137.3, 136.6, 136.4, 136.3, 135.0, 134.5, 134.2, 129.4, 129.0, 128.9, 128.8, 126.0, 123.4, 120.4, 119.9, 110.6, 110.6 (Ar–*C*), 23.8, 21.5 (Mes–*CH*$_3$). ^{11}B NMR (CD_2Cl_2): δ +84.9 (s, br). ^{31}P NMR (CD_2Cl_2): δ −12.4 (s). Anal. Calcd for $C_{48}H_{43}BNP$: C, 85.33; H, 6.41; B, N, 2.07. Found: C, 84.98; H, 6.32; N, 2.02. mp = 235 °C.

9-(2-(Diisopropylphosphino)-5-(dimesitylboryl)phenyl)-9*H*-carbazole (C*zm*BPi, 2b)

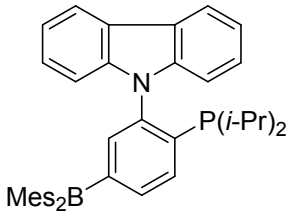

This compound was prepared in a manner analogous to the synthesis of **1b** using **2a** (0.38 g, 0.87 mmol), *n*-BuLi (0.35 mL, 0.87 mmol), and Mes_2BF (0.24 g, 0.89 mmol) to give C*zm*BPi (**2b**) as a white powder (Yield: 0.33 g, 63%). Single crystals suitable for an X-ray diffraction study were obtained by slow evaporation of a mixed solution of **2b** in acetonitrile/CH_2Cl_2, affording colorless crystals. ^{1}H NMR (CD_2Cl_2): δ 8.10 (d, J = 7.3 Hz, 2H), 7.77 (dd, J = 7.7, 1.7 Hz, 1H), 7.62 (dd, J = 7.7, 1.3 Hz, 1H), 7.40 (dd, J = 3.6, 0.9 Hz, 1H), 7.34 (td, J = 7.8, 1.2 Hz, 2H), 7.22 (td, J = 7.4, 0.9 Hz, 2H), 6.96 (d, J = 8.2 Hz, 2H, Ar–*H*), 6.79 (s, 4H) (Mes–*H*), 2.24 (s, 6H, Mes–CH_3), 2.02 (s, 12H, Mes–CH_3), 2.00–1.93 (m, 2H, isopropyl–C*H*), 1.00–0.76 (m, 12H, isopropyl–CH_3). ^{13}C NMR (CD_2Cl_2): δ 143.7, 143.4, 143.0, 142.7, 142.7, 142.6, 141.8, 141.3, 139.8, 137.0, 136.9, 135.8, 134.5, 134.4, 128.9, 126.0, 123.3, 120.6, 119.9, 111.1, 111.0 (Ar–*C*), 25.0, 24.8 (isopropyl–*C*), 23.8, 21.5 (Mes–*C*), 20.7, 20.5, 20.3, 20.1 (isopropyl–*C*). ^{11}B NMR (CD_2Cl_2): δ +83.9 (s, br). ^{31}P NMR (CD_2Cl_2): δ −5.4 (s). Anal. Calcd for $C_{42}H_{47}BNP$: C, 83.02; H, 7.80; N, 2.31. Found: C, 82.93; H, 7.82; N, 2.30. mp = 211 °C.

9-(5-(Dimesitylboryl)-2-(diphenyloxophosphino)phenyl)-9*H*-carbazole (C*zm*BPO, 1c)

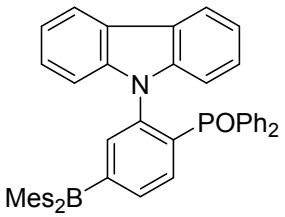

To a solution of **1b** (0.14 g, 2.08 mmol) in CH_2Cl_2 (5 mL) was added dropwise H_2O_2 (30% in water, 1 mL, 8.82 mmol) at room temperature. The reaction mixture was stirred for 6 h, extracted with CH_2Cl_2 (5 mL × 3), and washed with water (10 mL × 3). The combined organic layer was dried over $MgSO_4$, filtered, and concentrated under reduced pressure. The crude product was purified by silica gel column chromatography using ethyl acetate/CH_2Cl_2 (1:10, v/v) as an eluent to give C*zm*BPO

(**1c**) as a greenish yellow powder (Yield: 0.10 g, 78%). ^{1}H NMR (CD_2Cl_2): δ 7.95 (dd, J = 13.0, 7.7 Hz, 1H), 7.79 (d, J = 7.6 Hz, 2H), 7.73 (d, J = 7.6 Hz, 1H), 7.43 (d, J = 4.7 Hz, 1H), 7.40–7.25 m, 6H), 7.21–7.10 (m, 4H), 7.01 (td, J = 7.6, 3.0 Hz, 4H), 6.89 (d, J = 8.1 Hz, 2H), 6.78 (s, 4H, Mes–*H*), 2.25 (s, 6H, Mes–CH_3), 2.04 (s, 12H, Mes–CH_3). ^{13}C NMR ($CDCl_3$): δ 142.0, 140.7, 139.6, 139.5, 139.4, 138.1, 138.0, 138.0, 136.8, 135.54, 135.4, 135.3, 131.9, 131.0, 131.98, 130.0, 130.8, 130.5, 128.5, 127.7, 127.5, 125.3, 123.0, 119.5, 110.4 (Ar–*C*), 23.5, 21.2 (Mes–*CH*$_3$). ^{11}B NMR (CD_2Cl_2): δ +79.5 (s, br). ^{31}P NMR (CD_2Cl_2): δ +27.0 (s). Anal. Calcd for $C_{48}H_{43}BNOP$: C, 83.35; H, 6.27; N, 2.03. Found: C, 83.20; H, 6.36; N, 1.97. mp = 132 °C.

9-(2-(Diisopropyloxophosphino)-5-(dimesitylboryl)phenyl)-9*H*-carbazole (C*zm*BPiO, 2c)

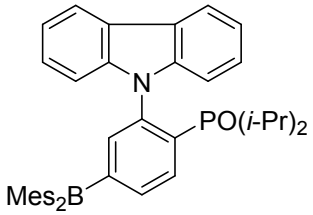

This compound was prepared in a manner analogous to the synthesis of **1c** using **2b** (0.20 g, 0.34 mmol) and H_2O_2 (30% in water, 1 mL, 8.82 mmol) to give C*zm*BPiO (**2c**) as a greenish yellow powder (Yield: 0.14 g, 70%). Single crystals suitable for an X-ray diffraction study were obtained by slow evaporation of a mixed solution of **2c** in acetonitrile/CH_2Cl_2, affording yellow crystals. ^{1}H NMR (CD_2Cl_2): δ 8.10 (d, J = 7.6 Hz, 2H), 8.04 (dd, J = 7.8, 2.7 Hz, 1H), 7.74 (d, J = 7.7 Hz, 1H), 7.36 (t, J = 6.9 Hz, 3H), 7.25 (t, J = 7.4 Hz, 2H), 6.88 (d, J = 8.1 Hz, 2H), 6.78 (s, 4H, Mes–*H*), 2.23 (s, 6H, Mes–*CH*$_3$), 2.00 (s, 12H, Mes–*CH*$_3$), 1.83 (septet, J = 6.9 Hz, 2H, isopropyl–C*H*), 1.03–0.89 (m, 12H, isopropyl–CH_3). ^{13}C NMR (CD_2Cl_2): δ 143.8, 141.3, 140.4, 140.4, 140.1, 139.0, 138.9, 137.4, 136.4, 136.1, 136.0, 134.9, 134.8, 128.9, 126.2, 123.7, 120.8, 120.2, 110.6 4 (Ar–*C*), 28.3, 27.5 (isopropyl–*C*), 23.8, 21.5 (Mes–*C*), 18.0, 17.9, 16.3, 16.2 (isopropyl–*C*). ^{11}B NMR (CD_2Cl_2): δ +83.5 (s, br). ^{31}P NMR (CD_2Cl_2): δ +50.3 (s). Anal. Calcd for $C_{42}H_{47}BNOP{\cdot}H_2O$: C, 78.62; H, 7.70; N, 2.18. Found: C, 78.68; H, 7.53; N, 2.20. mp = 215 °C.

9-(3-(Dimesitylboranyl)phenyl)-9*H*-carbazole (C*zm*B)

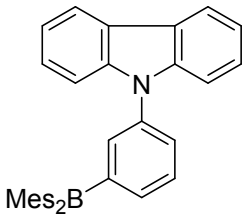

This compound was prepared in a manner analogous to the synthesis of **1b** using 9-(3-bromophenyl)-9*H*-carbazole (0.20 g, 0.62 mmol), *n*-BuLi (0.30 mL, 0.75 mmol), and Mes_2BF (0.18 g, 0.67 mmol) to give C*zm*B as a yellow powder (Yield: 0.22 g, 72%). Single crystals suitable for an X-ray diffraction study were obtained by slow evaporation of a mixed solution of C*zm*B in CH_3OH/CH_2Cl_2, affording pale yellow crystals. ^{1}H NMR ($CDCl_3$): δ 8.10 (d, J = 7.8 Hz, 2H), 7.65–7.56 (m, 4H), 7.39–7.34 (m, 2H), 7.28–7.22 (m, 4H), 6.80 (s, 4H) (Mes–*H*), 2.26 (s, 6H, Mes–CH_3), 2.06 (s, 12H, Mes–CH_3). ^{13}C NMR

($CDCl_3$): δ 141.11, 140.87, 139.24, 137.57, 135.09, 134.24, 130.65, 129.69, 128.49, 125.98, 123.35, 120.41, 119.89, 109.70 (Ar–*C*), 23.58, 21.37 (Mes–*C*). ^{11}B NMR ($CDCl_3$): δ +75.1 (s, br). Anal. Calcd for $C_{36}H_{34}BN$: C, 87.98; H, 6.97; N, 2.85. Found: C, 87.35; H, 7.05; N, 2.97.

1.3. X-ray crystallography

Single crystals of suitable size and quality were coated with Paratone oil and mounted onto a glass capillary. Diffractrion data were obtained at 173 K. The crystallographic measurements were performed on a Bruker SMART Apex II CCD area detector diffractometer with a graphite-monochromated Mo-Kα radiation (λ = 0.71073 Å). The structures were solved by direct methods and refined by full-matrix least-squares fitting on F^2 using SHELXL-2014.[1] All non-hydrogen atoms were refined with anisotropic displacement parameters. The carbon-bound hydrogen atoms were introduced at calculated positions and all hydrogen atoms were treated as riding atoms with an isotropic displacement parameter equal to 1.2 times that of the parent atom. Full details of the structure determinations have been deposited as a cif with the Cambridge Crystallographic Data Collection under CCDC deposition numbers 1855527 (**2b**, Cz*m*BPi), 1855528 (**2c**, Cz*m*BPiO), and 1855529 (Cz*m*B). The data can be obtained free of charge via www.ccdc.cam.ac.uk/data_request/cif.

1.4. Cyclic voltammetry

Cyclic voltammetry measurements were carried out in acetonitrile (MeCN, 1×10^{-3} M) with a three-electrode cell configuration consisting of platinum working and counter electrodes and an $Ag/AgNO_3$ (0.01 M in CH_3CN) reference electrode at room temperature. Tetra-*n*-butylammonium hexafluorophosphate (0.1 M) was used as the supporting electrolyte. The redox potentials were recorded at a scan rate of 100 mV/s and are reported with reference to the ferrocene/ferrocenium (Fc/Fc^+) redox couple.

1.5. Photophysical measurements

UV/vis absorption and photoluminescence (PL) spectra were recorded on a Varian Cary 100 and FS5 spectrophotometer, respectively. Solution PL spectra were obtained from oxygen-free and air-saturated solutions. Oxygen-free solvent was prepared by degassing of the spectroscopic-grade solvent for ca. 30 min and kept in a nitrogen-filled glovebox. Dilute sample solutions (typically 5.0×10^{-5} M) were prepared in a glovebox at ambient conditions. Absolute photoluminescence quantum yields (PLQYs, Φ_{PL}) of solutions were measured on an absolute PL quantum yield spectrophotometer (Quantaurus-QY

C11347-11, Hamamatsu Photonics) equipped with a 3.3 inch integrating sphere. Transient PL decays were measured on an FS5 spectrophotometer (Edinburgh Instruments) in either time-correlated single-photon counting (TCSPC) mode (an EPL-375 picosecond pulsed diode laser or an EPLED-330 picosecond pulsed LED laser as a light source) or multi-channel scaling (MCS) mode (a microsecond Xenon flashlamp as a light source). The lifetimes of prompt fluorescence (τ_p) were estimated by fitting decay curves measured via the TCSPC mode, while those of delayed fluorescence (τ_d) were estimated with curves measured via the MCS mode. PLQYs of prompt (Φ_{PF}) and delayed (Φ_{DF}) fluorescence were estimated from the prompt and delayed components of the transient decay curves, respectively. The temperature-dependence of PL decay was obtained with an OptistatDN^{TM} cryostat (Oxford Instruments). The HOMO and LUMO energy levels were determined from the electrochemical oxidation (E_{onset}) and reduction ($E_{1/2}$) peaks of the cyclic voltammograms. Time-resolved emission spectra (TRES) were recorded on an FS5 spectrophotometer with 375-nm or 330-nm laser excitaion. TRES measurements were performed using a degassed ethanolic solution containing a phosphine oxide sample (**1c** or **2c**) and a competitive organic fluorescent dye (typically 0.5–2.0 μM of fluorescein disodium salt or rhodamine B). The progress of oxidation reaction of phosphine (**2b**) to phosphine oxide (**2c**) was monitored by in situ steady-state PL measurements of the dilute ethanolic sample solutions (1.0×10^{-5} M) in the presence of excess (10 equiv) H_2O_2 at different temperatures. In situ TRES measurements were conducted using a degassed ethanolic solution containing a mixture of phosphine (**2b**), fluorescent dye, and excess (10 equiv) H_2O_2 after heating at 50 °C for 30 min.

1.6. Theoretical calculations

All calculations were performed using the Gaussian 09 program package.[2] The geometry optimization of ground states was computed with density functional theory (DFT) at the M062X/6-31g(d) levels,[3] and the energy minima were confirmed by the calculation with zero imaginary mode of vibrations. The calculated absorptions and emissions were obtained using the time-dependent density functional theory (TD-DFT) method within the Tamm–Dancoff approximation,[4] taking the optimized geometries at S_0 and S_1 states, respectively. The ground state optimized geometry was used for the investigation of the vertical excitation and the optimized geometries at lowest singlet and triplet excited states were used for the calculation of ΔE_{ST}. All the calculations are performed in toluene using polarizable continuum model (PCM).[5] The overlap integral extents were computed using Multiwfn program.[6]

1.7. References

1. Sheldrick, G. M. *Acta Crystallogr. A* **2008**, *64*, 112-122; Sheldrick, G. M. *Acta Crystallogr., Sect. C* **2015**, *C71*, 3-8.

2. Frisch, M. J.; Trucks, G. W.; Schlegel, H. B.; Scuseria, G. E.; Robb, M. A.; Cheeseman, J. R.; Scalmani, G.; Barone, V.; Mennucci, B.; Petersson, G. A.; Nakatsuji, H.; Caricato, M.; Li, X.; Hratchian, H. P.; Izmaylov, A. F.; Bloino, J.; Zheng, G.; Sonnenberg, J. L.; Hada, M.; Ehara, M.; Toyota, K.; Fukuda, R.; Hasegawa, J.; Ishida, M.; Nakajima, T.; Honda, Y.; Kitao, O.; Nakai, H.; Vreven, T.; Montgomery, J. A., Jr.; Peralta, J. E.; Ogliaro, F.; Bearpark, M.; Heyd, J. J.; Brothers, E.; Kudin, K. N.; Staroverov, V. N.; Keith, T.; Kobayashi, R.; Normand, J.; Raghavachari, K.; Rendell, A.; Burant, J. C.; Iyengar, S. S.; Tomasi, J.; Cossi, M.; Rega, N.; Millam, J. M.; Klene, M.; Knox, J. E.; Cross, J. B.; Bakken, V.; Adamo, C.; Jaramillo, J.; Gomperts, R.; Stratmann, R. E.; Yazyev, O.; Austin, A. J.; Cammi, R.; Pomelli, C.; Ochterski, J. W.; Martin, R. L.; Morokuma, K.; Zakrzewski, V. G.; Voth, G. A.; Salvador, P.; Dannenberg, J. J.; Dapprich, S.; Daniels, A. D.; Farkas, Ö.; Foresman, J. B.; Ortiz, J. V.; Cioslowski, J.; Fox, D. J. , *Gaussian 09, Revision E.01*.; Gaussian, Inc.: Wallingford, CT, 2013.

3. Zhao, Y.; Truhlar, D. G. *J. Phys. Chem. A* **2006**, *110*, 13126-13130.

4. Hirata, S.; Head-Gordon, M. *Chem. Phys. Lett*. **1999**, *314*, 291–299.

5. Tomasi, J.; Mennucci, B.; Cammi, R. *Chem. Rev*. **2005**, *105*, 2999-3094.

6. Lu, T.; Chen, F. *J. Comput. Chem*. **2012**, *33*, 580-592.

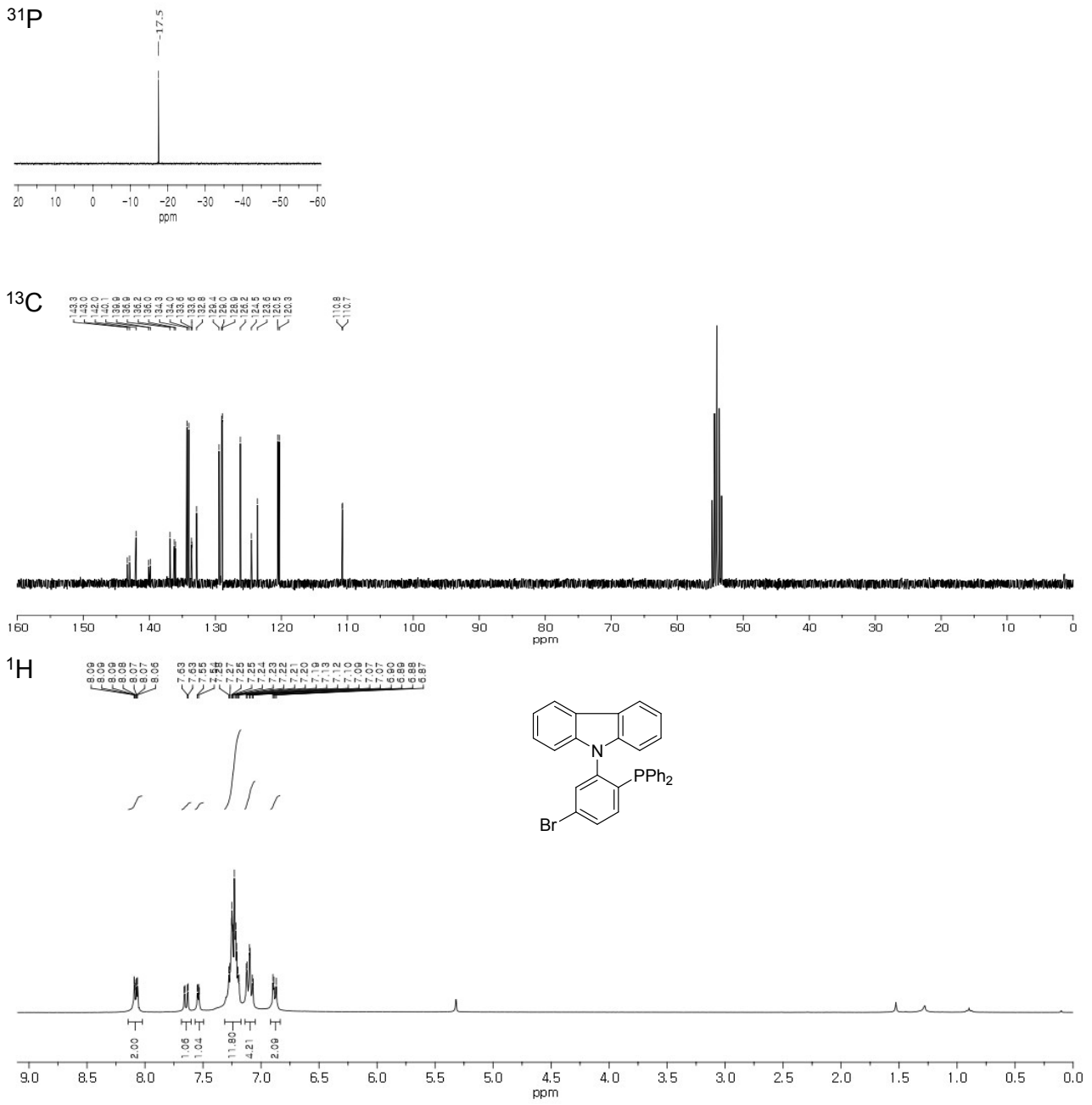

Fig. S1. NMR spectra of **1a** in CD_2Cl_2.

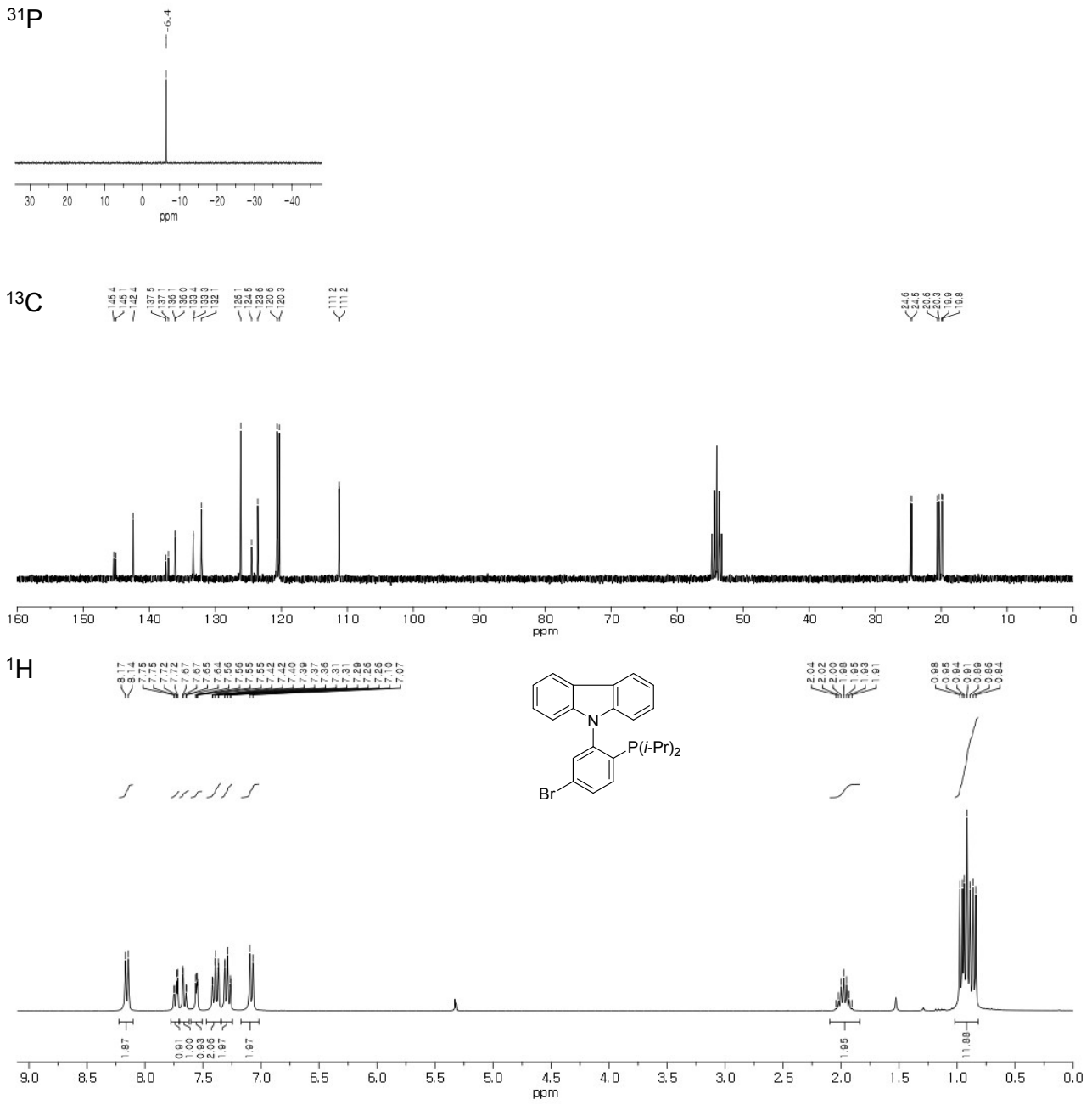

Fig. S2. NMR spectra of **2a** in CD_2Cl_2.

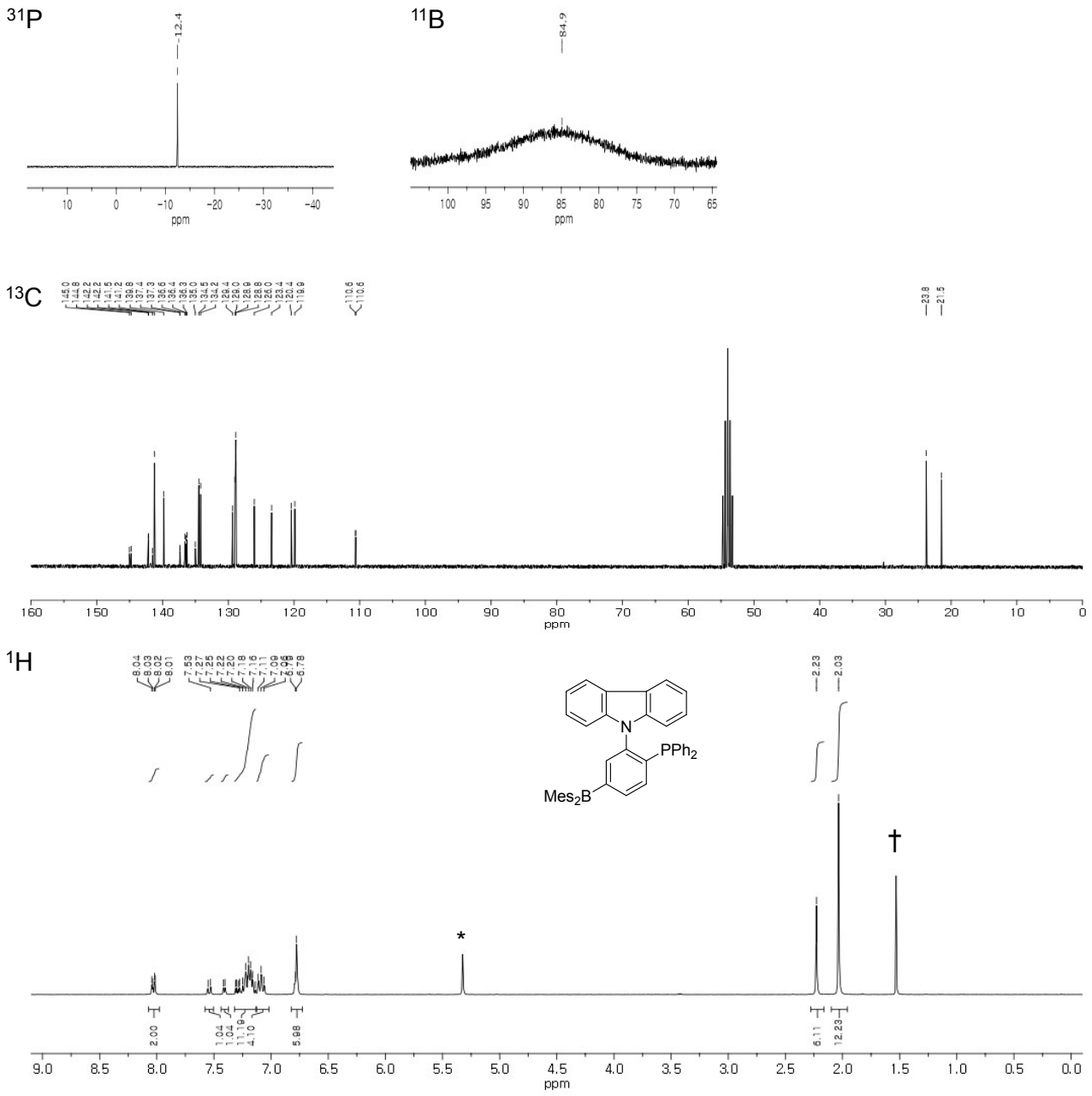

Fig. S3. NMR spectra of C*z*m*BP* (**1b)** in CD_2Cl_2 (* and † from residual $CHDCl_2$ and H_2O, respectively).

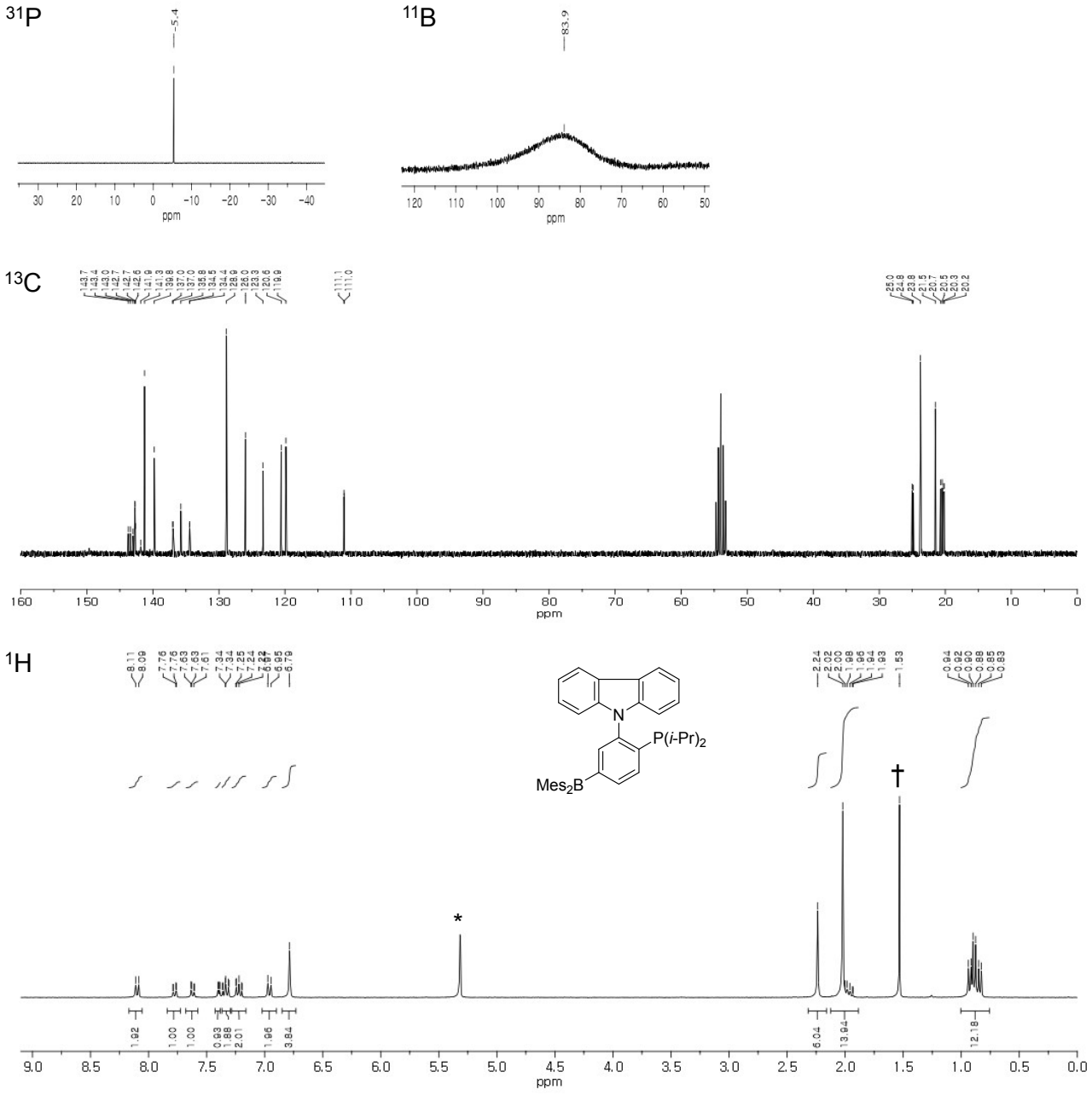

Fig. S4. NMR spectra of Cz*m*BPi (**2b)** in CD_2Cl_2 (* and † from residual $CHDCl_2$ and H_2O, respectively).

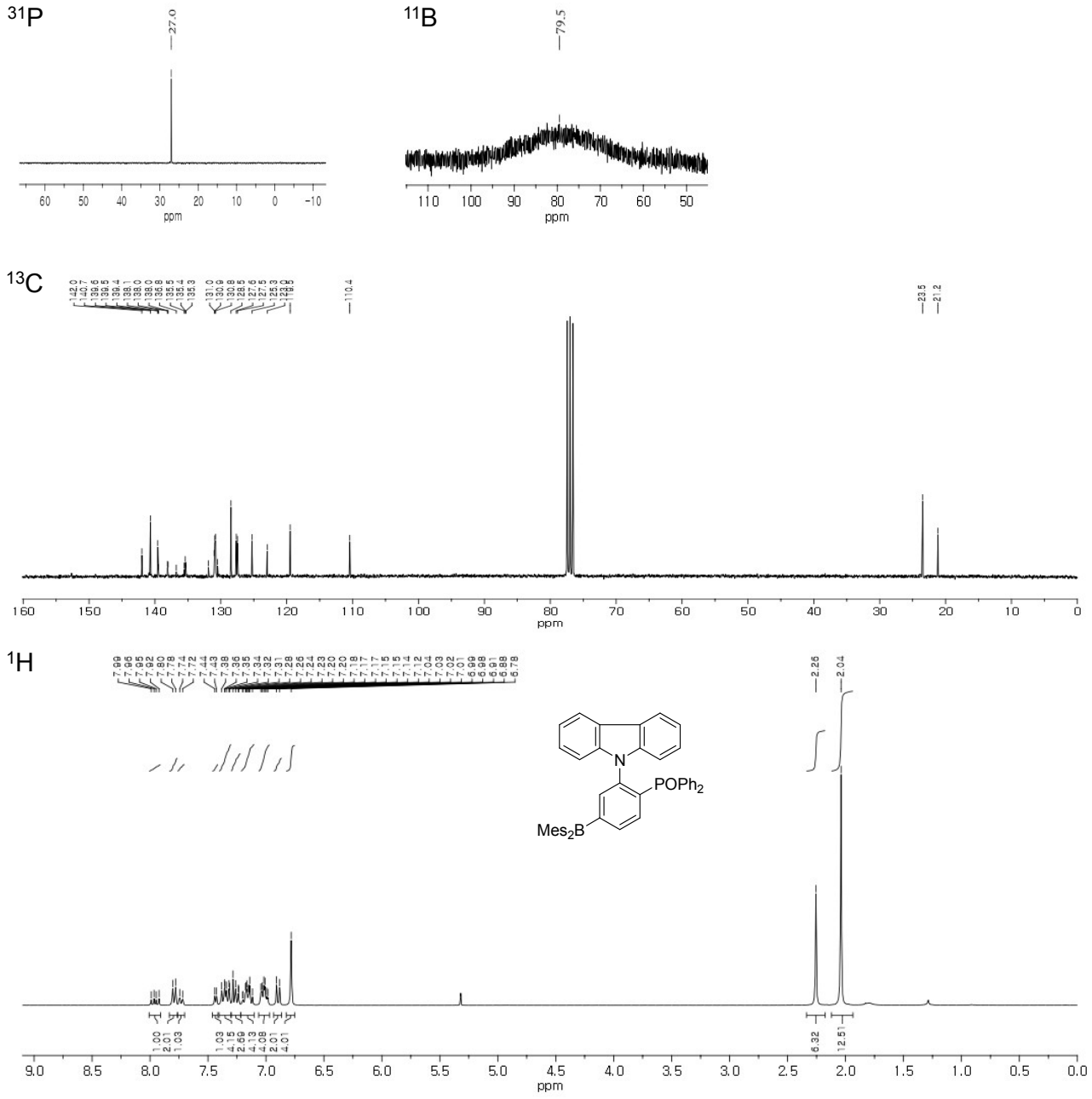

Fig. S5. NMR spectra of Cz*m*BPO (**1c)** in CD_2Cl_2.

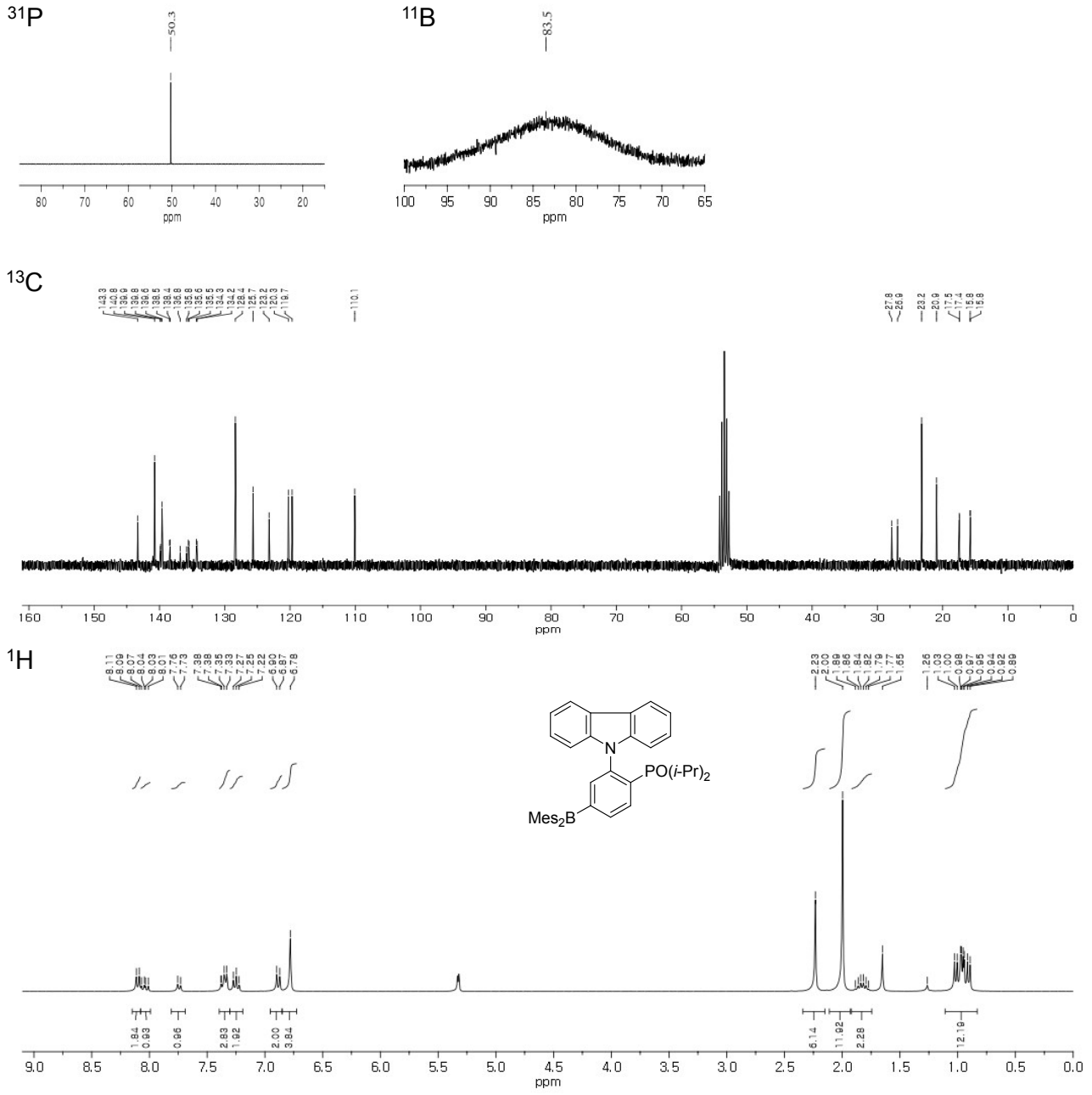

Fig. S6. NMR spectra of Cz*m*BPiO (**2c)** in CD_2Cl_2.

Table S1. Crystallographic data and parameters for **2b**, **2c**, and Cz*m*B.

	Cz*m*BPi (**2b**)	Cz*m*BPiO·CH_3CN (**2c** ·CH_3CN)	Cz*m*B
formula	$C_{42}H_{47}BNP$	$C_{44}H_{50}BN_2OP$	$C_{36}H_{34}BN$
formula weight	607.58	664.64	491.45
crystal system	Orthorhombic	Monoclinic	monoclinic
space group	Pbca	$P2_1/c$	$P2_1/c$
a (Å)	16.4464(3)	8.76940(10)	15.7787(2)
b (Å)	18.2277(3)	26.1702(3)	8.2376(2)
c (Å)	24.0228(3	17.0409(2)	21.5820(3)
α (°)	90	90	90
β (°)	90	95.5961(8)	100.2920(10)
γ (°)	90	90	90
V (Å^3)	7201.6(2)	3892.20(8)	2760.06(9)
Z	8	4	4
ρ_{calc} (g cm^{-3})	1.121	1.134	1.183
μ (mm^{-1})	0.105	0.105	0.067
F(000)	2608	1424	1048
T (K)	173(2)	173(2)	173(2)
hkl range	−10→+21, −24→+24, −32→+31	−11→+10, −31→+34, −22→+22	−20→+20, −10→+10, −27→+28
measd reflns	39480	38927	25167
unique reflns [R_{int}]	8886 [0.0561]	9601 [0.0480]	6309 [0.0415]
reflns used for refinement	8886	9601	6309
refined parameters	409	443	343
R1[a] (I > 2σ(I))	0.0601	0.0718	0.0597
wR2[b] all data	0.1788	0. 2243	0.1877
GOF on F^2	1.054	1.062	1.069
ρ_{fin} (max/min) (e Å^{-3})	0.847/−0.307	0.687/−0.440	0.454/−0.420

[a] $R1 = \sum||Fo| - |Fc||/\sum|Fo|$. [b] $wR2 = \{[\sum w(Fo^2 - Fc^2)^2]/[\sum w(Fo^2)^2]\}^{1/2}$.

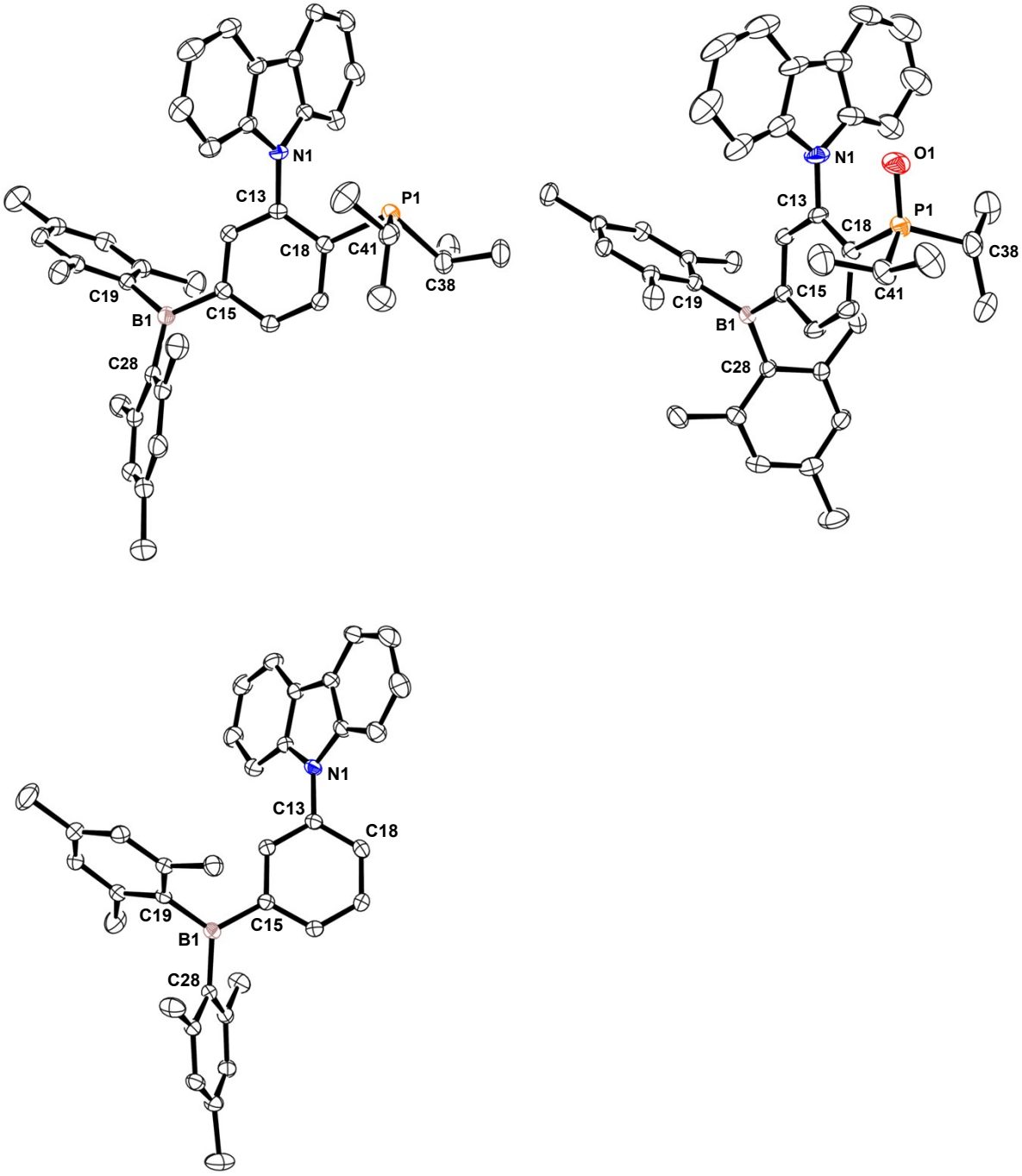

Fig. S7. Crystal structures of (top) **2b** (left) and **2c** (right) and (bottom) Cz*m*B (40% thermal ellipsoids) with atom labels. H atoms and a solvent molecule are omitted for clarity.

Table S2. Selected bond lengths (Å) and angles (deg) for **2b**, **2c**, and C*zm*B.

	2b	**2c**	C*zm*B
Lengths (Å)			
B(1)–C(28)	1.568(3)	1.572(3)	1.583(3)
B(1)–C(15)	1.573(3)	1.569(3)	1.572(3)
B(1)–C(19)	1.574(4)	1.571(3)	1.571(3)
N(1)–C(13)	1.431(2)	1.433(3)	1.419(2)
P(1) –C(18)	1.8526(19)	1.828(2)	–
P(1) –C(38)	1.854(2)	1.820(3)	–
P(1) –C(41)	1.862(2)	1.818(3)	–
P(1) –O(1)	–	1.4800(19)	–
Angles (°)			
C(28)–B(1)−C(15)	116.3(2)	116.31(19)	118.90(17)
C(28)–B(1)−C(19)	124.69(17)	125.71(19)	123.41(15)
C(15)–B(1)−C(19)	119.02(18)	117.96(18)	117.68(15)
N(1)–C(13)−C(18)	121.23(16)	121.9(2)	120.25(16)
C(13)–C(18)−P(1)	120.78(14)	124.42(17)	–

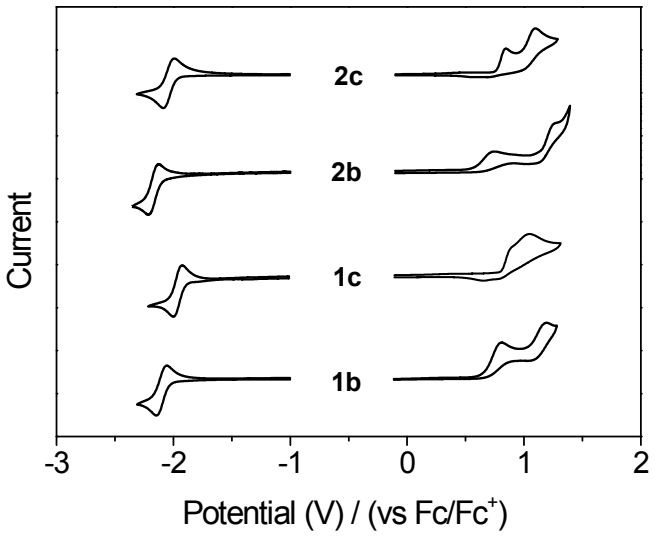

	E_{ox}^{onset} (V)	$E_{red}^{1/2}$ (V)
C*zm*BP (**1b**)	0.67	−2.10
C*zm*BPO (**1c**)	0.82	−1.95
C*zm*BPi (**2b**)	0.58	−2.17
C*zm*BPiO (**2c**)	0.77	−2.04

Fig. S8. Cyclic voltammograms of **1b–c** and **2b–c** (1.0×10^{-3} M in MeCN, scan rate = 100 mV/s).

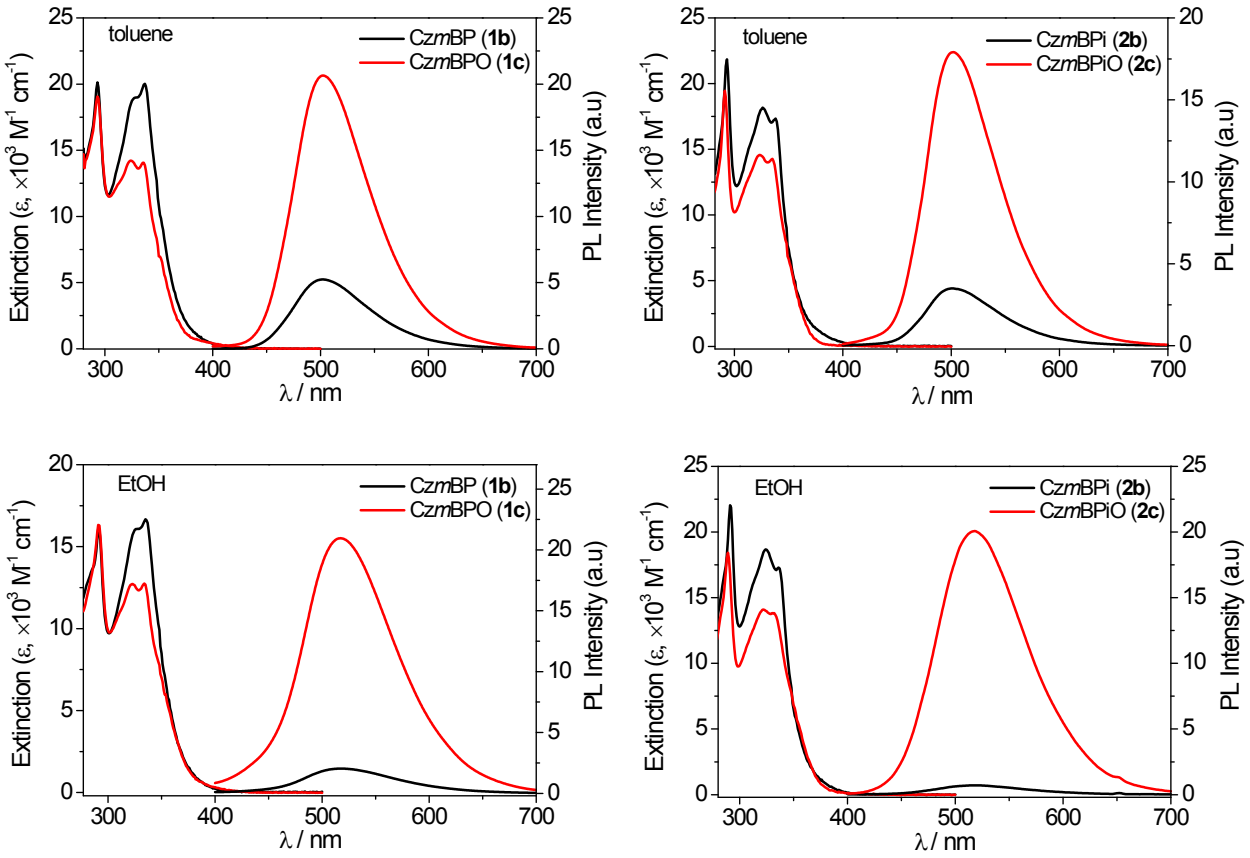

Fig. S9. UV/vis absorption and PL spectra of **1b–c** (left) and **2b–c** (right) in toluene (top) and in EtOH (bottom) at 298 K.

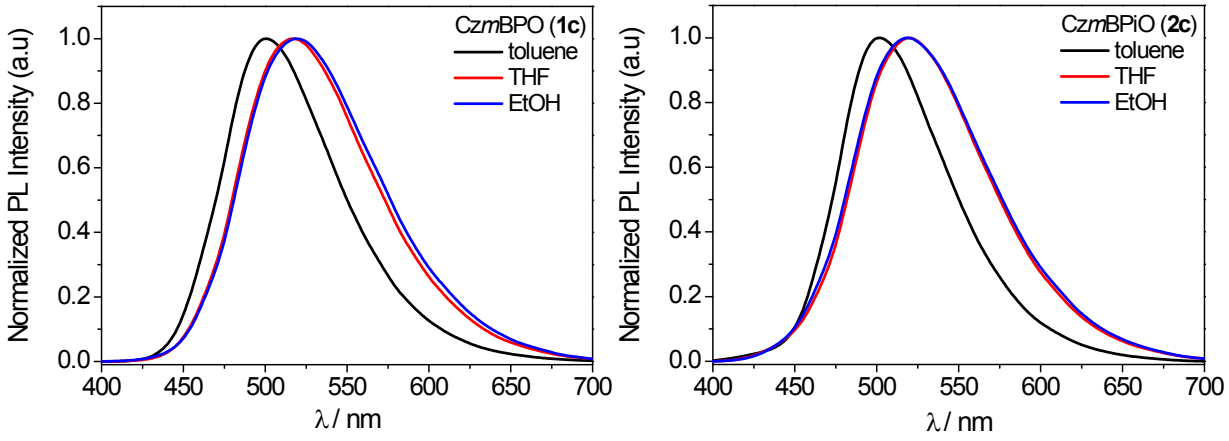

Fig. S10. PL spectra of **1c** and **2c** in solvents of different polarity at 298 K.

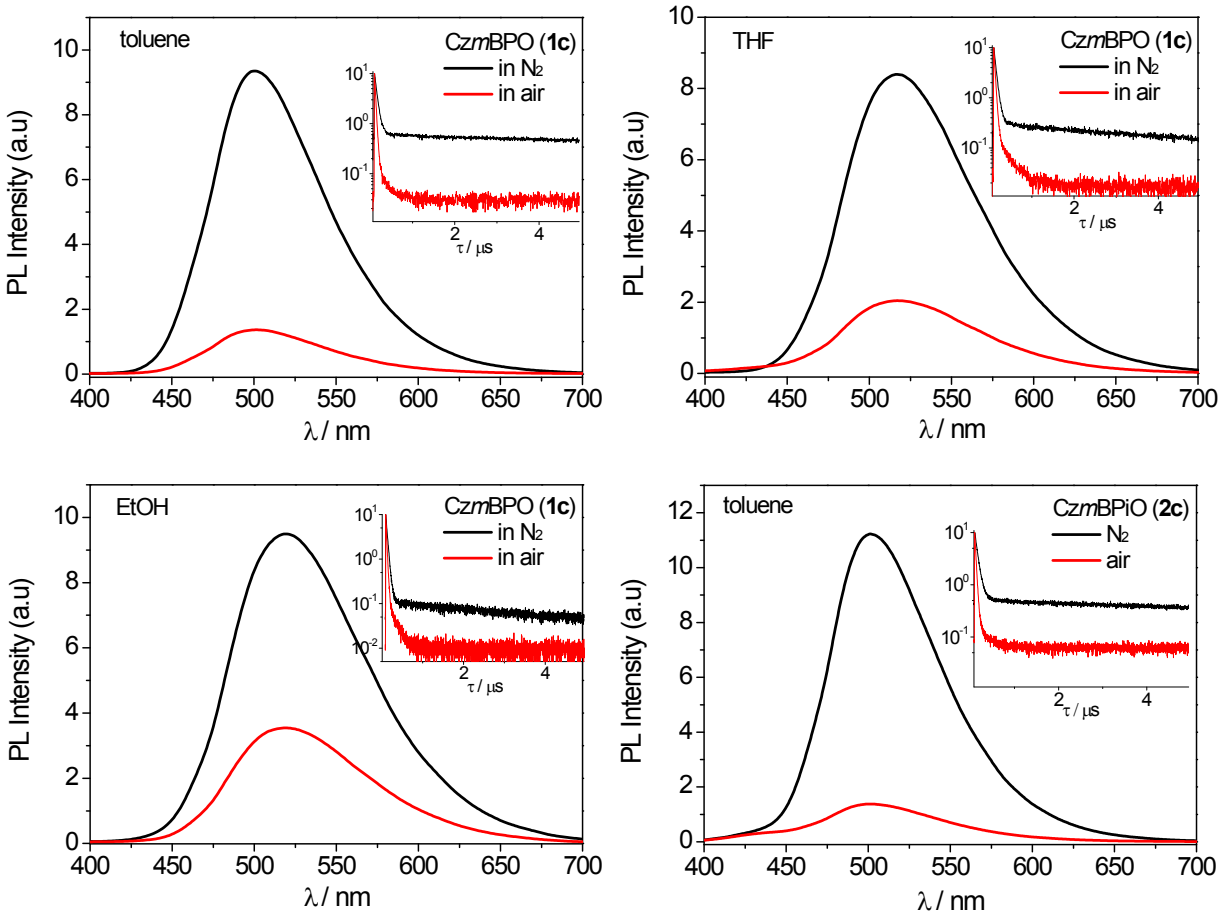

Fig. S11. PL spectra of **1c** and **2c** in oxygen-free (black line) and air-saturated (red line) solvents at 298 K. Insets: transient PL decay curves.

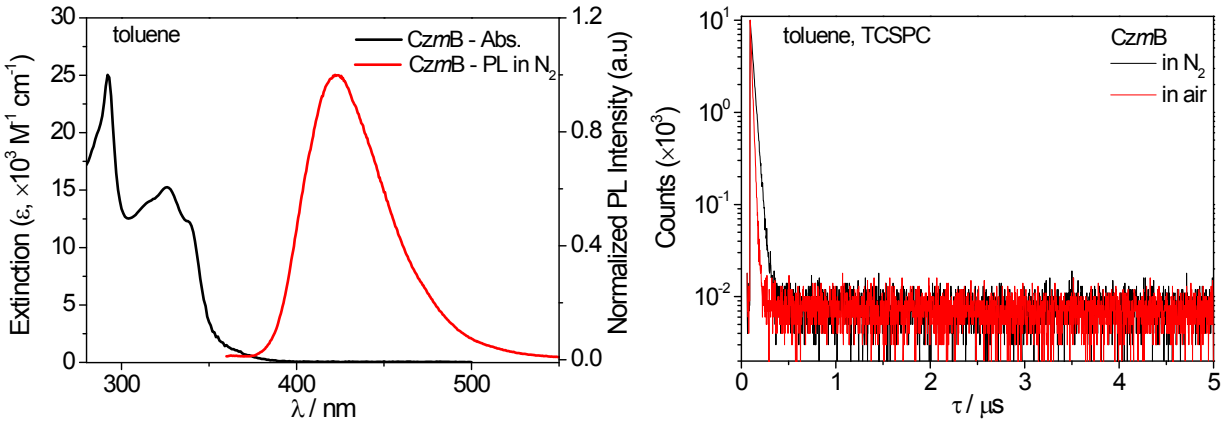

Fig. S12. (Left) UV/vis absorption and PL spectra and (right) transient PL decay curves of Cz*m*B in toluene (5.0×10^{-5} M) at 298 K. Photophysical data: λ_{abs} / nm (ε) = 292 (25.04), 326 (15.2), 338 (12.3, sh). λ_{PL} = 423 nm. τ (N_2) = 30.1 ns. Φ_{PL} (N_2) = 0.30.

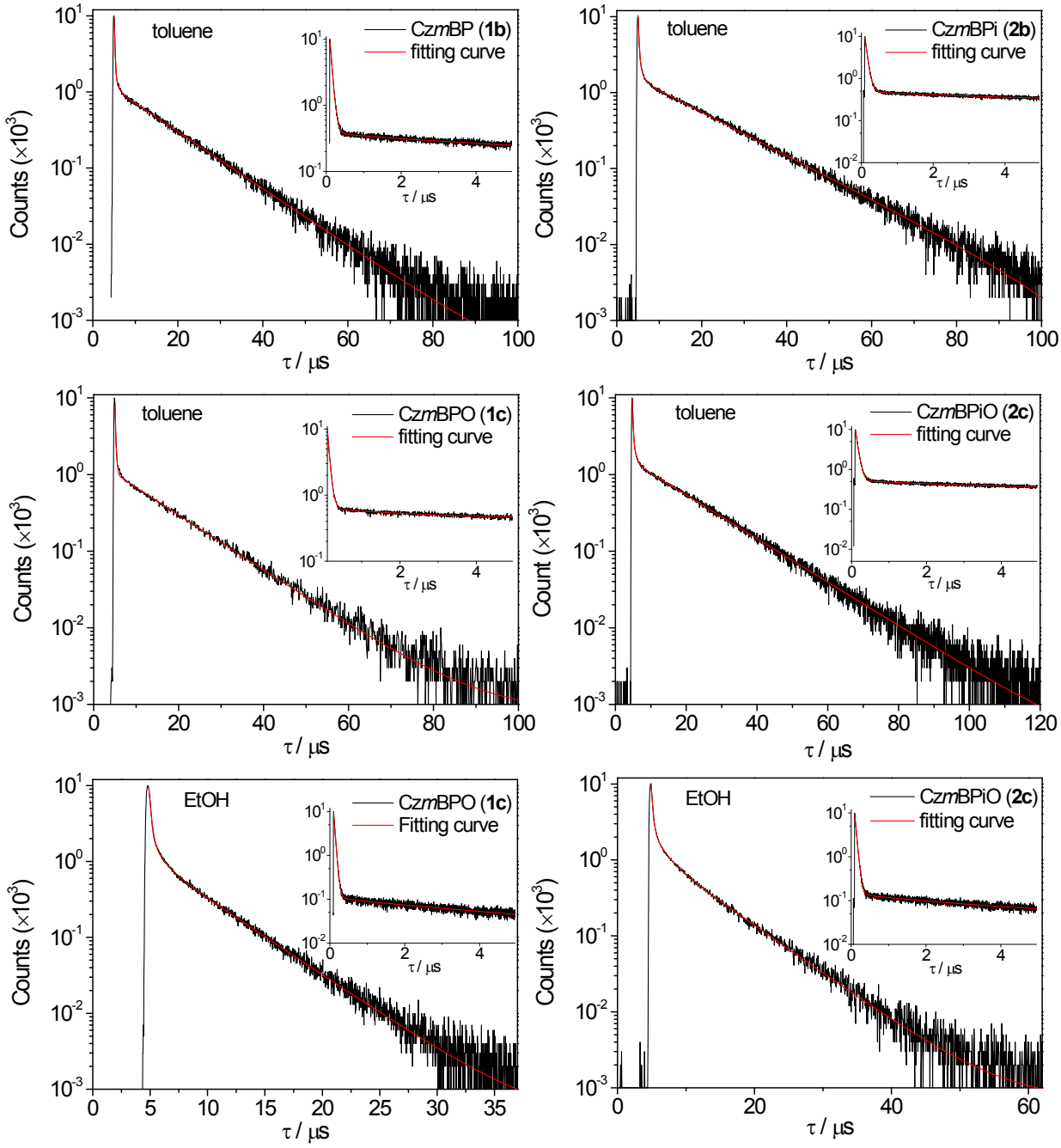

Fig. S13. Transient PL decay curves of **1b**–**2b** and **1c**–**2c** in oxygen-free solvents measured from the MCS mode at 298 K. Insets: decay curves from the TCSPC mode.

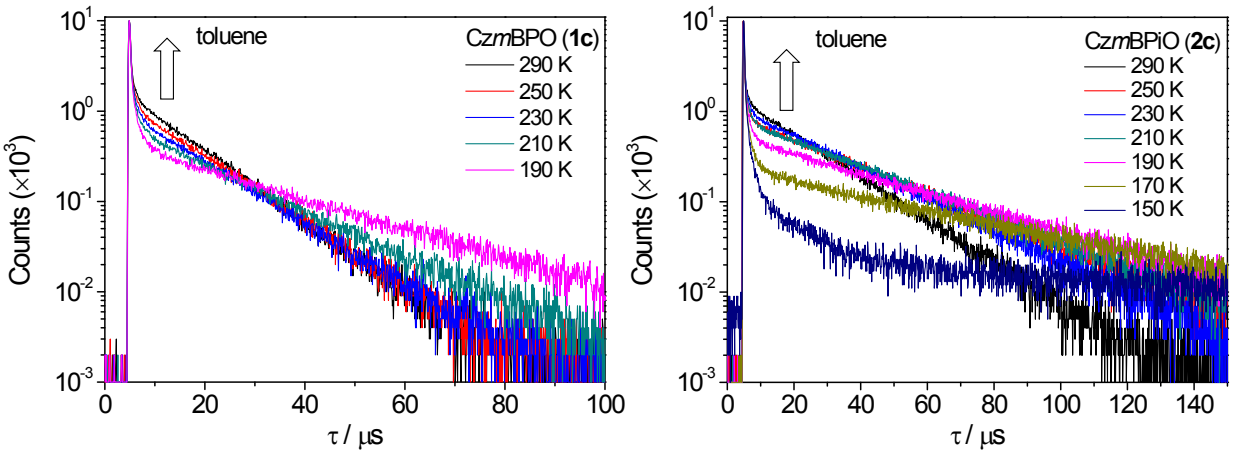

Fig. S14. Temperature dependence of transient PL decay of **1c** (left) and **2c** (right) in oxygen-free toluene.

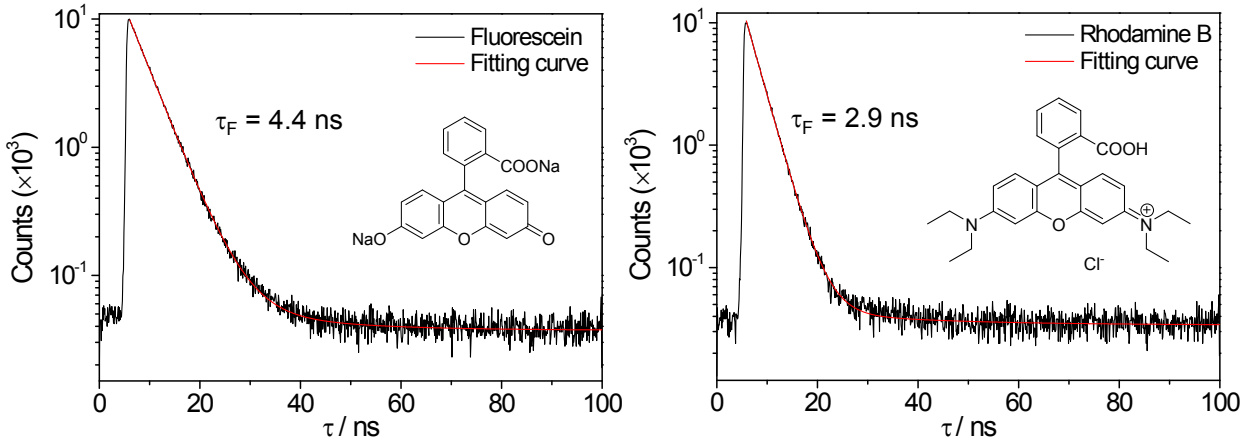

Fig. S15. Transient PL decay curves of fluorescein disodium salt (left) and rhodamine B (right) in oxygen-free EtOH at 298 K.

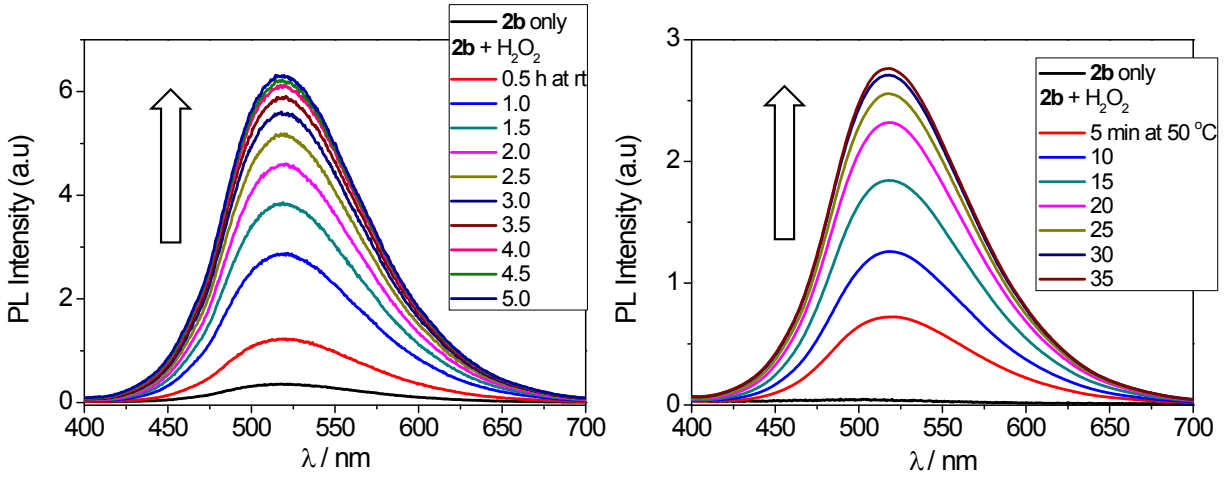

Fig. S16. In situ PL spectra of an ethanolic solution of **2b** in the presence of H_2O_2 (10 equiv) at RT (left) and 50 °C (right).

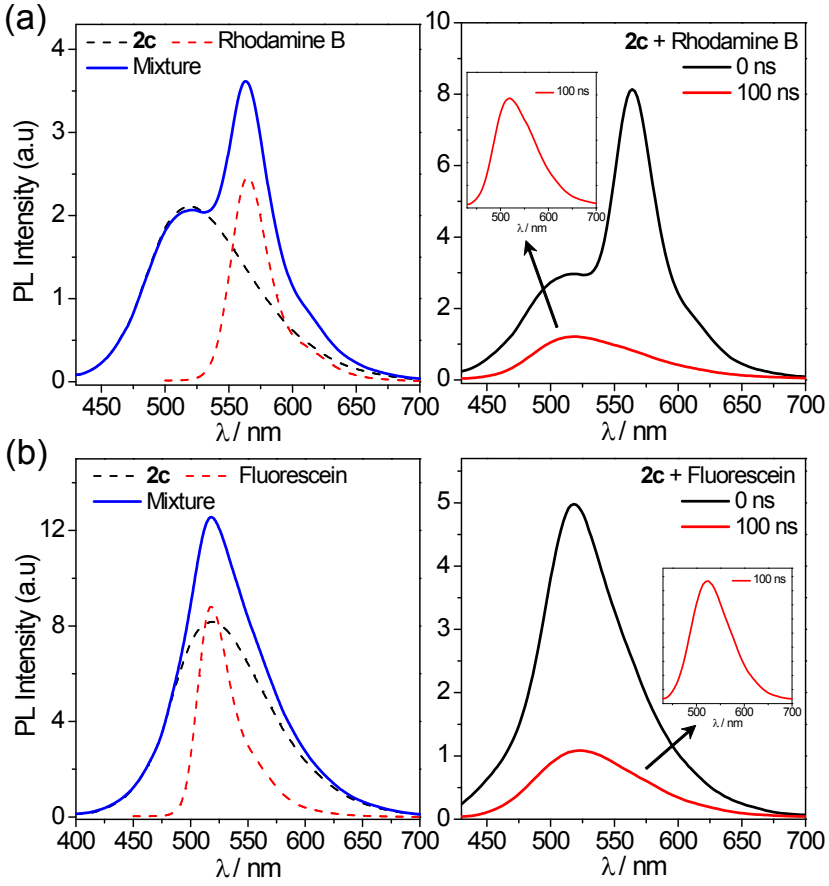

Fig. S17. (a) Steady-state PL spectra of **2c** (10 μM), rhodamine B (0.5 μM), and their mixture in EtOH (left) and TRES of an ethanolic solution containing **2c** (10 μM) and rhodamine B (0.5 μM) recorded after a 100 ns delay (right). λ_{ex}(laser) = 375 nm for TRES. (b) Steady-state PL spectra (left) and TRES (right) of **2c** (10 μM) in the presence of fluorescein disodium salt (2 μM). λ_{ex}(laser) = 330 nm for TRES.

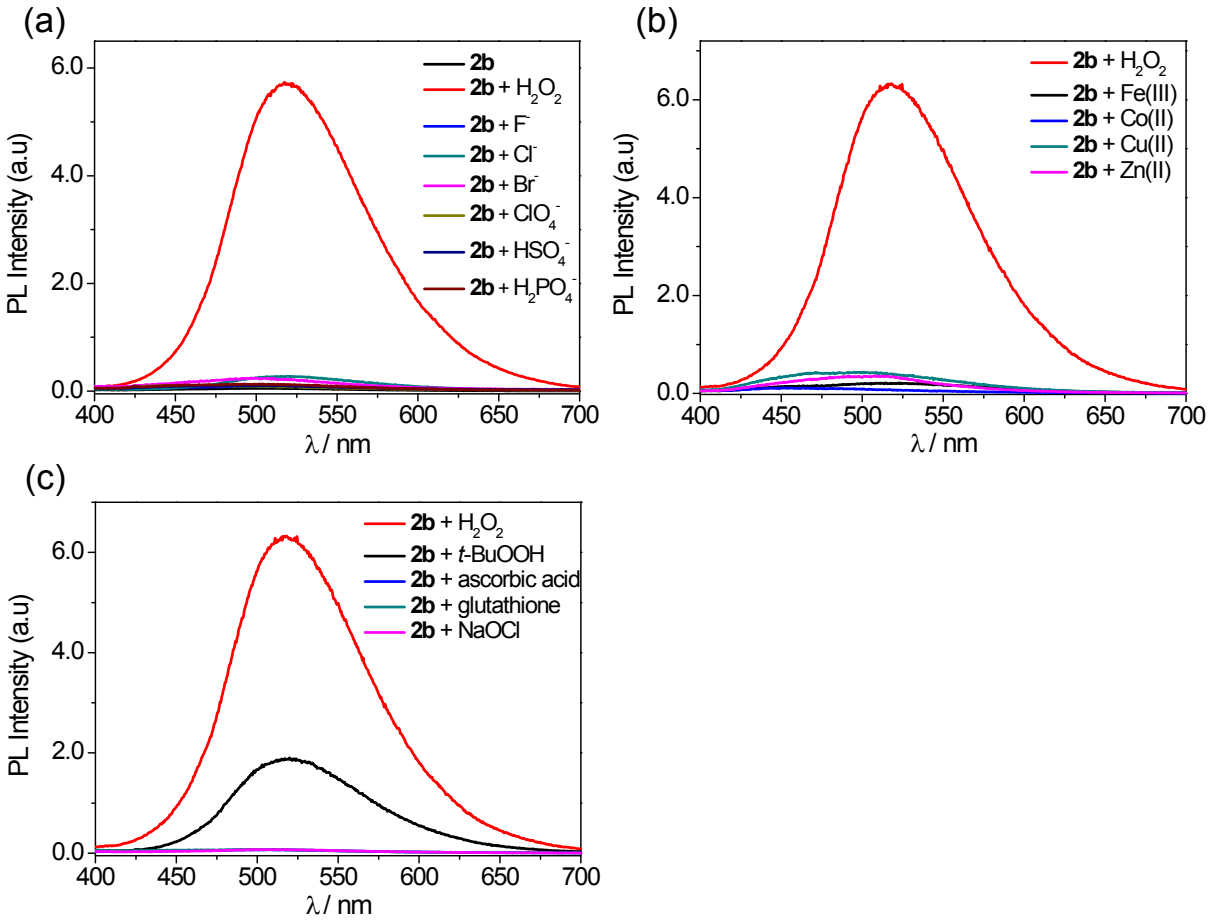

Fig. S18. PL spectra of **2b** (10 μM) in the presence of various analytes (10 equiv), (a) anions: F^-, Cl^-, Br^-, ClO_4^-, HSO_4^-, $H_2PO_4^-$ as tetrabutylammonium salts, (b) metal ions: Fe^{3+}, Co^{2+}, Cu^{2+}, Zn^{2+} as perchlorate salts, (c) biologically relevant species: NaOCl, *t*-BuOOH, ascorbic acid, glutathione, in oxygen-free EtOH. The spectra were acquired after 10 min reaction time at 298 K.

2. Computational results

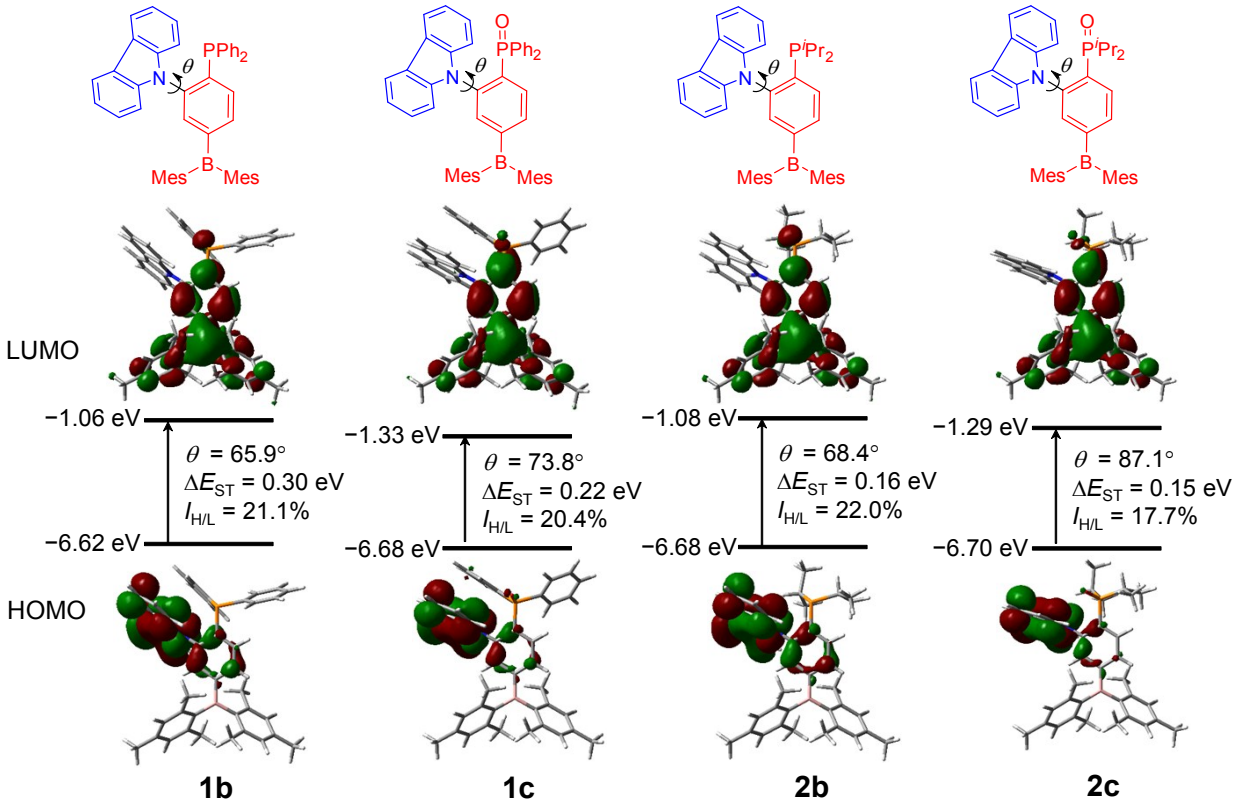

Fig. S19. The frontier molecular orbitals, HOMO and LUMO, of **1b–c** and **2b–c** (isovalue = 0.02) at their ground state (S_0) geometries from DFT calculations. The orbital energies, dihedral angles (θ), energy splitting between the S_1 and T_1 states (ΔE_{ST}), and overlap integral extents ($I_{H/L}$) are provided.

Table S3. Molecular orbital energies (in eV) and the contribution (in %) of donor and acceptor moieties to the frontier molecular orbitals at the ground state (S_0) optimized geometries and the overlap integral ($I_{H/L}$, in %) between HOMO and LUMO for **1b**–**2c**.

	MO	energy (eV)	donor (Cz)	acceptor (Mes_2BPh)	acceptor (R_2P or R_2PO)	$I_{H/L}$
1b (Cz*m*BP)	LUMO	−1.06	0.43	96.23	3.34	21.07
	HOMO	−6.62	91.42	7.76	0.82	
1c (Cz*m*BPO)	LUMO	−1.33	0.60	94.59	4.81	20.44
	HOMO	−6.68	93.28	5.56	1.16	
2b (Cz*m*BPi)	LUMO	−1.08	0.46	96.14	3.40	21.96
	HOMO	−6.68	91.20	8.26	0.54	
2c (Cz*m*BPiO)	LUMO	−1.29	0.49	95.94	3.57	17.73
	HOMO	−6.70	94.93	4.5	0.57	

Table S4. The computed absorption wavelength (λ_{abs}, in nm), corresponding oscillator strength (*f*), and major contribution for the transition in **1b**–**2c**.

	λ_{abs}	*f*	major contribution
1b (Cz*m*BP)	314	0.136	HOMO→LUMO (61%)
			HOMO-3→LUMO (29%)
1c (Cz*m*BPO)	334	0.059	HOMO→LUMO (86%)
			HOMO-3→LUMO (29%)
2b (Cz*m*BPi)	314	0.206	HOMO→LUMO (50%)
			HOMO-3→LUMO (27%)
			HOMO-1→LUMO (12%)
2c (Cz*m*BPiO)	328	0.061	HOMO→LUMO (78%)
			HOMO-2→LUMO (13%)

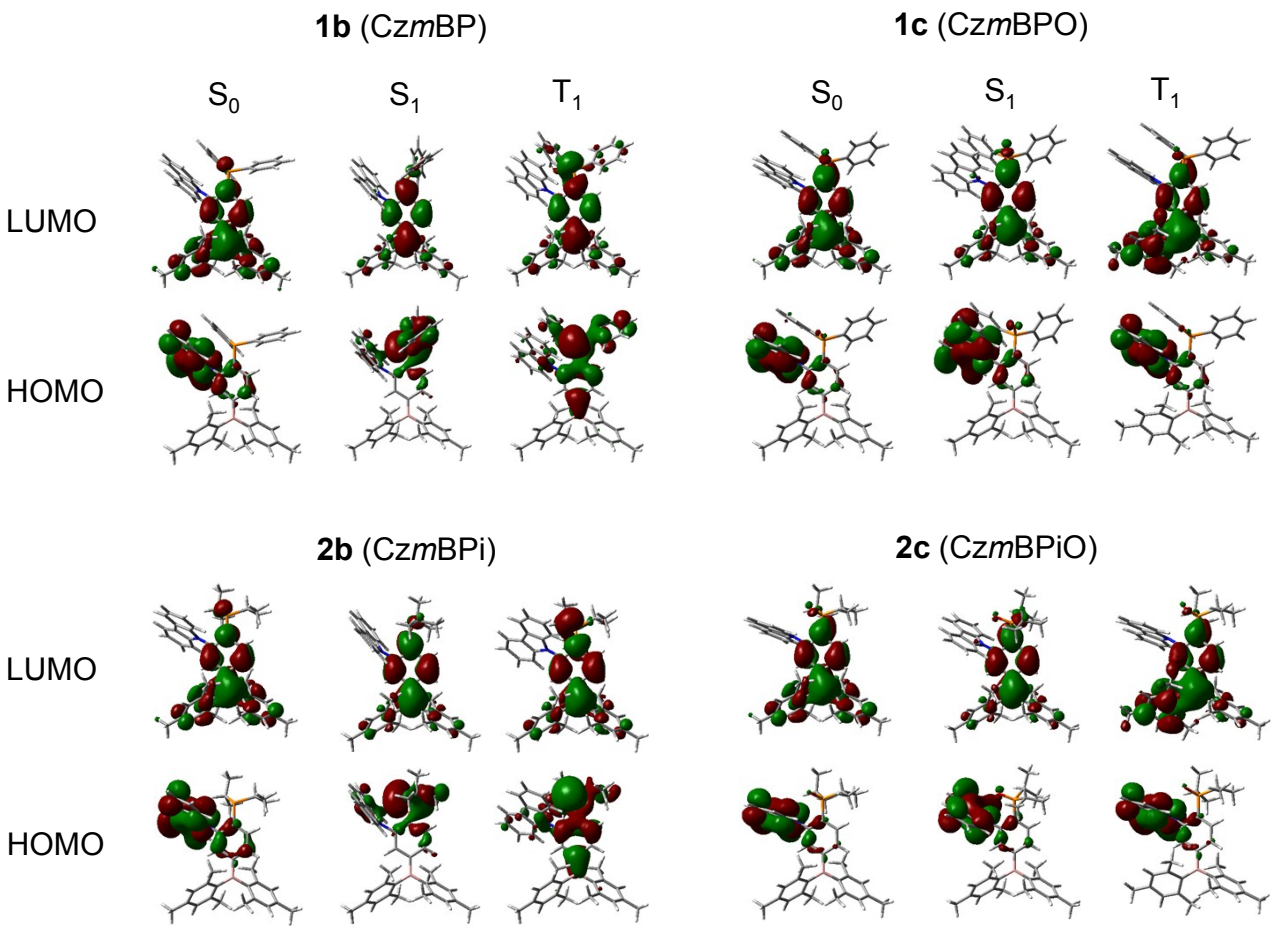

Fig. S20. The frontier molecular orbitals, HOMO and LUMO, of **1b–c** and **2b–c** (isovalue = 0.02) at their S_0, S_1, and T_1 optimized geometries.

Table S5. The computed vertical emission wavelength (λ_{em} in nm) from singlet excited state (S_1) with the corresponding oscillator strength (f) and reorganization energy (λ_{ROE}) in **1b**–**2c**.

	λ_{em}	f	λ_{ROE} (eV)
1b (Cz*m*BP)	656	0.006	0.27
1c (Cz*m*BPO)	404	0.035	0.09
2b (Cz*m*BPi)	732	0.001	0.47
2c (Cz*m*BPiO)	425	0.012	0.19